

## **Supplementary Material**

# **Bismuth Decorated Honeycomb-like Carbon Nanofibers: An Active Electrocatalyst for Construction of Sensitive Nitrite Sensor**

**Fengyi Wang<sup>1,2</sup>, Ye Li<sup>2</sup>, Chenglu Yan<sup>3</sup>, Qiuting Ma<sup>2</sup>, Xiaofeng Yang<sup>1\*</sup>, Huaqiao Peng<sup>3</sup>, Huiyong Wang<sup>4</sup>, Juan Du<sup>2\*</sup>, Baozhan Zheng<sup>2\*</sup> and Yong Guo<sup>2</sup>**

<sup>1</sup> Institute of Quality Standard and Testing Technology for Agro-products of Sichuan Academy of Agricultural Sciences, Chengdu 610066, China.

<sup>2</sup> College of Chemistry, Sichuan University, No. 29 Wangjiang Road, Chengdu 610064, China.

<sup>3</sup> The Second Research Institute of Civil Aviation Administration of China, Chengdu 610041, China.

<sup>4</sup> College of Chemistry and Chemical Engineering, Henan Normal University, Henan 453002, China.

\* Correspondence: yangxiaofeng\_cd@sina.com (X. Yang); dujuanchem@scu.edu.cn (J. Du); zhengbaozhan@scu.edu.cn (B. Zheng).

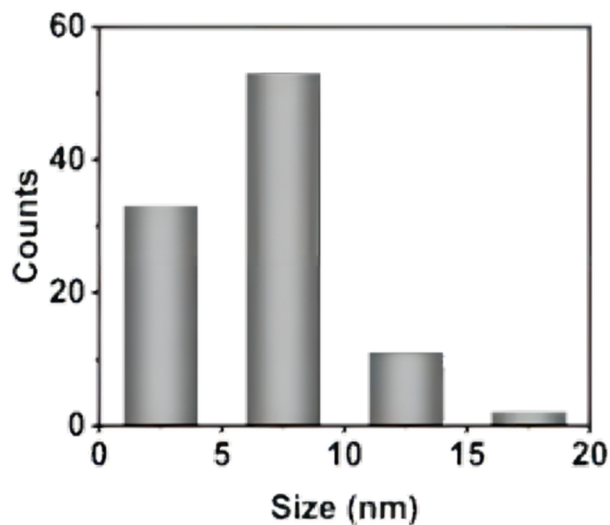


**Figure S1.** particle size distribution histograms of Bi NPs on the surface of HCNFs.

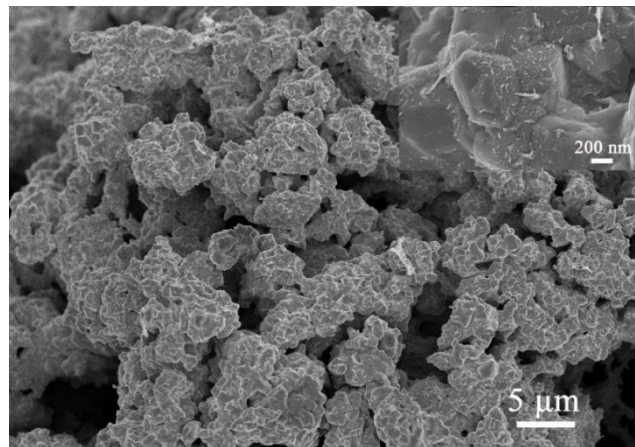


**Figure S2.** The SEM image of Bi NPs (inset of Figure S2 high magnification SEM image).

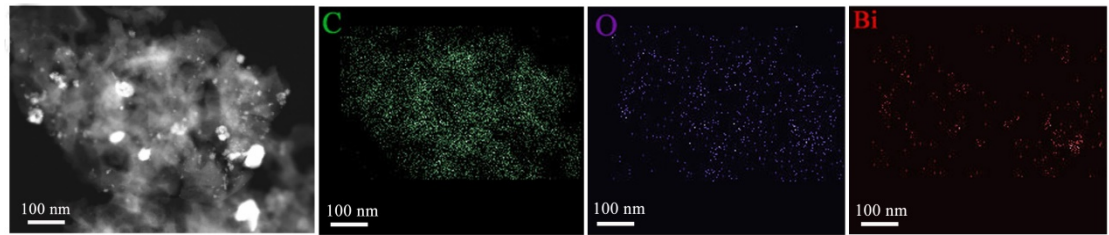


**Figure S3.** STEM image and corresponding elemental mapping images of Bi, C, O for Bi/HCNFs, respectively.

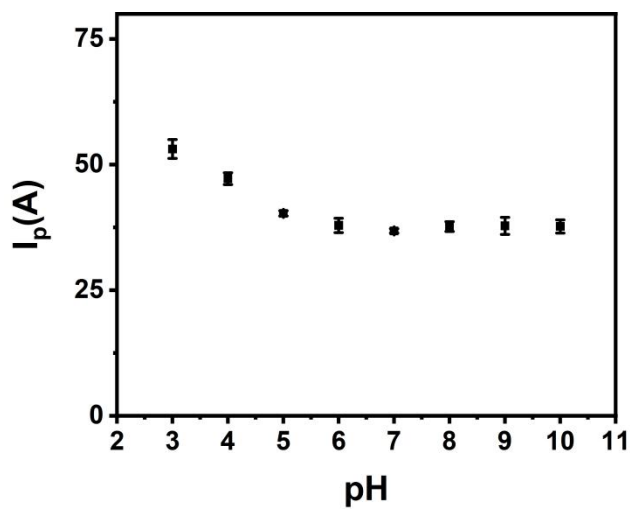


**Figure S4.** The diagram of CV peak current and pH in the presence of 1 mM  $\text{NO}_2^-$  ranging from 3.0 to 10.0.

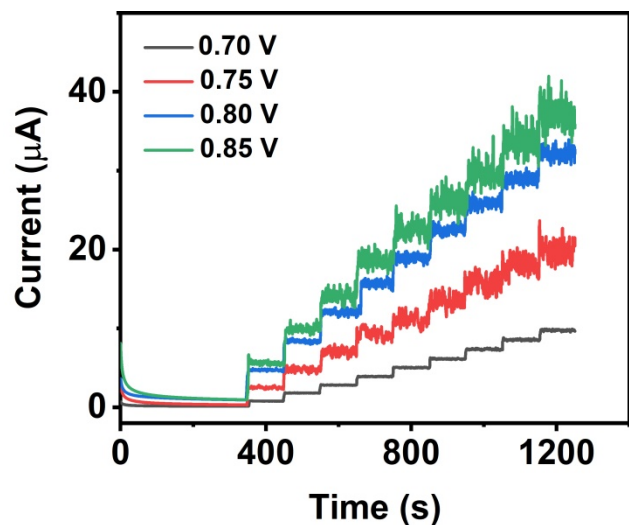


**Figure S5.** The amperometric responses of Bi/HCNFs at different potentials of 0.70-0.85 V vs. Ag/AgCl with successive additions of 0.2 mM nitrite.

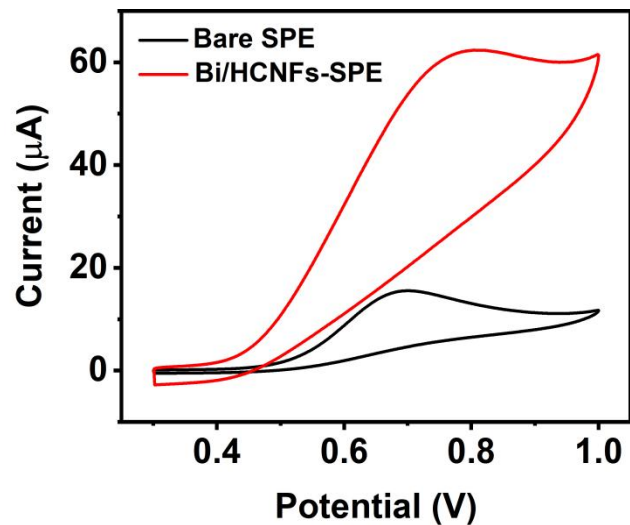


**Figure S6.** CV responses of disposable bare SPE and Bi/HCNFs modified SPE in 0.1 M PBS (pH 7.0) with the presence of 1 mM  $\text{NO}_2^-$ .

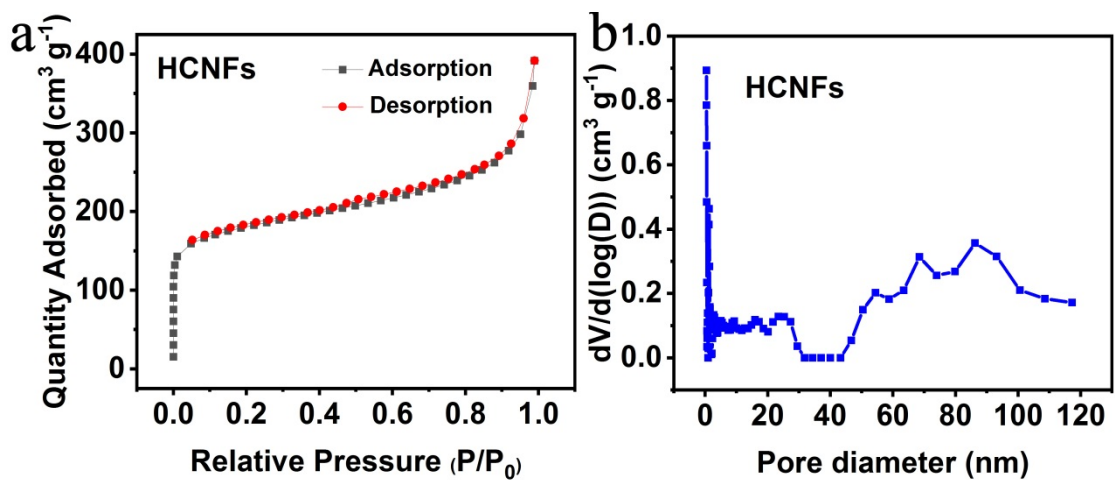


**Figure S7.** (a) Nitrogen adsorption-desorption isotherms of HCNFs and (b) its corresponding pore size distribution.

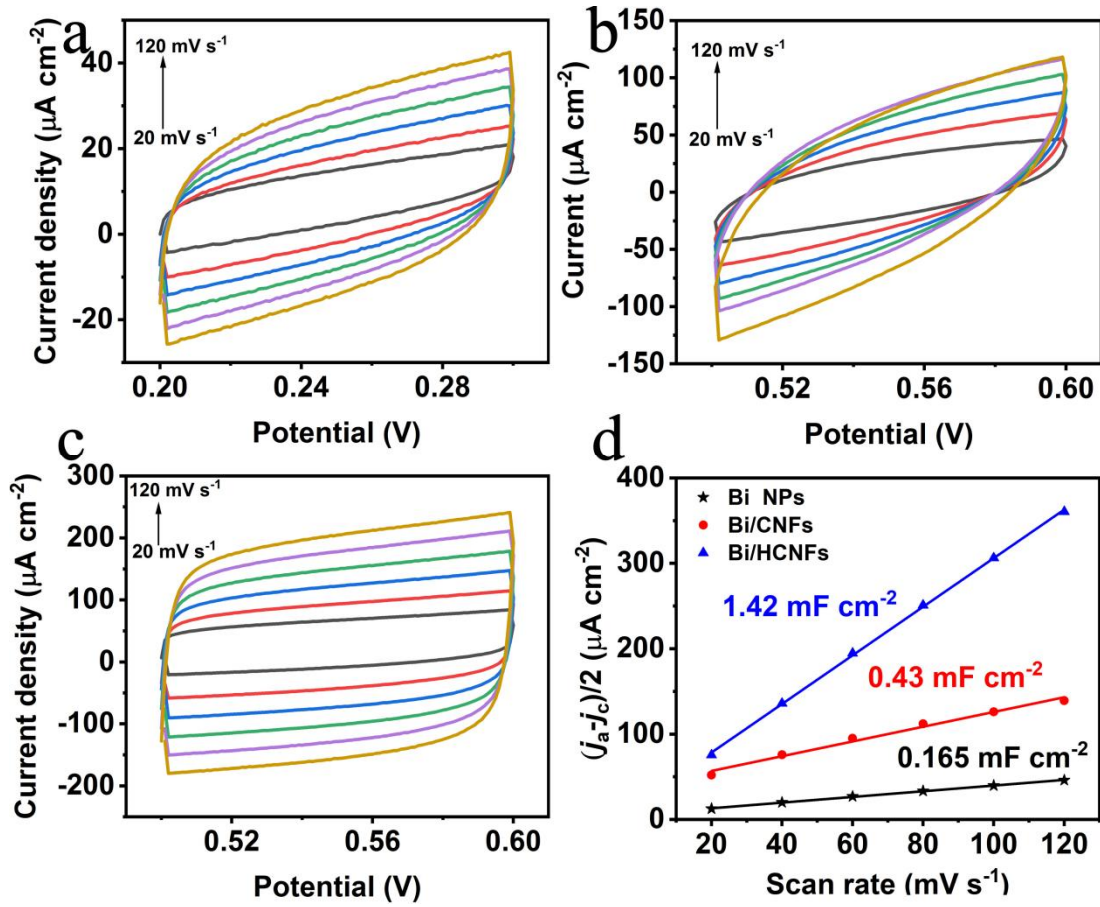


**Figure S8.** CV curves of Bi NPs (a), Bi/CNFs (b) and Bi/HCNFs (c) at different scan rates from 20 to 120  $\text{mV s}^{-1}$  in the region without faradaic current. (d) Plot of corresponding capacitive current densities of Bi NPs, Bi/CNFs and Bi/HCNFs with scan rates,  $j_a$  and  $j_c$  are the current densities of the anodic and cathodic branch of CV at a defined potential, respectively.



**Figure S9.** The photo of commercial screen-printed microelectrode with a drop of solution containing nitrite (200  $\mu$ L).

**Table S1.** Comparison of electrocatalytic performance toward nitrite with previous electrochemical sensors.

Electrode materials	LOD ( $\mu\text{M}$ )	Sensitivity ( $\mu\text{A mM}^{-1} \text{cm}^{-2}$ )	Reference
NiFe <sub>2</sub> O <sub>4</sub> NPs	0.1236	7961.7	[1]
NiFe-LDH NSAs/CC	0.02	803.6	[2]
Cu-MOF/Au	0.082	252	[3]
Ag/HNTs/MoS <sub>2</sub>	0.7	89.9 $\mu\text{A}/\text{mM}$	[4]
SnO <sub>2</sub> /Pt/Ti/SiO <sub>2</sub>	1.7	22.56 $\mu\text{A}/\text{mM}$	[5]
$\alpha$ -Fe <sub>2</sub> O <sub>3</sub> /CNTs hybrids	0.15	334	[6]
Fe <sub>3</sub> O <sub>4</sub> /rGO	0.3	226	[7]
Cu/MWNTs	1.8	455.84	[8]
TMPyPcCo/aCNTs	0.071	8 $\mu\text{A}/\text{mM}$	[9]
Bi/HCNFs	0.019	1269.9	This work

**Table S2.** Analysis results of trace nitrite in real samples on Bi/HCNFs-SPE through dropping tests (200  $\mu$ L).

Samples	Added ( $\mu$ M)	Found ( $\mu$ M)	Recovery (%)	<sup>a</sup> RSD(%)
Tap water	500	526.8	105.4	0.89
	1000	1038	103.8	1.62
Pickles	500	514.7	102.9	0.34
	1000	1059	105.9	0.78
Sausage	500	515.3	103.0	1.71
	1000	1053	105.3	0.76

<sup>a</sup>RSD: Relative standard deviation.

## References

1. Nithyayini, K.N.; Harish, M.N.K.; Nagashree, K.L. Electrochemical detection of nitrite at NiFe<sub>2</sub>O<sub>4</sub> nanoparticles synthesised by solvent deficient method. *Electrochim. Acta* **2019**, *317*, 701–710.
2. Ma, Y.; Wang, Y.; Xie, D.; Gu, Y.; Zhang, H.; Wang, G.; Zhang, Y.; Zhao, H.; Wong, P.K. NiFe-layered double hydroxide nanosheet arrays supported on carbon cloth for highly sensitive detection of nitrite. *ACS Appl. Mater. Interfaces* **2018**, *10*, 6541–6551.
3. Chen, H.; Yang, T.; Liu, F.; Li, W. Electrodeposition of gold nanoparticles on Cu-based metal-organic framework for the electrochemical detection of nitrite. *Sens. Actuators B: Chem.* **2019**, *286*, 401–407.
4. Ghanei-Motlagh, M.; Taher, M.A. A novel electrochemical sensor based on silver/halloysite nanotube/molybdenum disulfide nanocomposite for efficient nitrite sensing. *Biosens. Bioelectron.* **2018**, *109*, 279–285.
5. Lete, C.; Chelu, M.; Marin, M.; Mihaiu, S.; Preda, S.; Anastasescu, M.; Calderón-Moreno, J.M.; Dinulescu, S.; Moldovan, C.; Gartner, M. Nitrite electrochemical sensing platform based on tin oxide films. *Sens. Actuators B: Chem.* **2020**, *316*, 128102.
6. Wang, K.; Wu, C.; Wang, F.; Liu, C.; Yu, C.; Jiang, G. In-situ insertion of carbon nanotubes into metal-organic frameworks-derived  $\alpha$ -Fe<sub>2</sub>O<sub>3</sub> polyhedrons for highly sensitive electrochemical detection of nitrite. *Electrochim. Acta* **2018**, *285*, 128–138.
7. Teymourian, H.; Salimi, A.; Khezrian, S. Fe<sub>3</sub>O<sub>4</sub> magnetic nanoparticles/reduced graphene oxide nanosheets as a novel electrochemical and bioelectrochemical sensing platform. *Biosens. Bioelectron.* **2013**, *49*, 1–8.
8. Manoj, D.; Saravanan, R.; Santhanakshmi, J. Agarwal, S.V. Gupta, K.; Boukherroub, R. Towards green synthesis of monodisperse Cu nanoparticles: An efficient and high sensitive electrochemical nitrite sensor. *Sens. Actuators B: Chem.* **2018**, *266*, 873–882.
9. Zhang, J.; Zhang, Z.; Wu, H.; Wu, F.; He, C.; Wang, B.; Wu, Y.; Ren, Z. An electrochemical bifunctional sensor for the detection of nitrite and hydrogen peroxide based on layer-by-layer multilayer films of cationic phthalocyanine cobalt(II) and carbon nanotubes. *J. Mater. Chem. B* **2016**, *4*, 1310–1317.